Resin Based 3D Printing for Fabricating Reactive Porous Media

Salek[1], Md Fahim; Shinde[2], Vinita V.; Beckingham[2], Bryan S.; Beckingham[*2], Lauren E.

[1]Department of Civil & Environmental Engineering, Auburn University, Auburn, AL

[2]Department of Chemical Engineering, Auburn University, Auburn, AL

*Corresponding author (Email:leb0071@auburn.edu)

Key Words: Digital Light Projection 3D printing, Reactive porous media, Accessible surface area

Abstract

Resin based three-dimensional (3D) printing is popular for many applications including replicating geologic porous media samples. This study is the first to explore resin-based 3D printing of reactive porous media. Here, digital light projection (DLP) 3D printing of sandstone replicates was performed using photosensitive resin mixed with calcite of varying amounts. Printed samples were imaged in 3D using X-ray micro computed tomography (μCT). Printed sample porosities are consistent and close to the original mesh porosity. Calcite volume fractions are generally in agreement with the calcite content in the resin mixture. Calcite accessible surface areas are similar to published values for real sandstones and calcite dissolution was observed in acidic batch experiments, evidence of its surface reactivity. DLP printing is thereby promising for fabricating reactive porous media samples.

1 Introduction

3D printing of porous media has shown utility for replicating pore networks in undisturbed soil and rock samples [1-4], exploring hydraulic properties [5] and studying rock mechanics [6,7]. However, exploration of 3D printing for understanding reactive mineral systems in porous media remains limited.

Geochemical reaction rates are poorly understood due to inherent sample heterogeneity [8]. Even samples collected from the same formation have varying pore network structures and minerology [9]. 3D printing of reactive porous media would enable controlled investigation of geochemical reactions for varying conditions.

3D printing microparticles in resin has been studied for various applications [10,11], but not for fabrication of reactive porous media. Printing reactive porous media was first explored using calcite containing filaments using Fused Filament Fabrication (FFF) [12]. Accessible calcite surface area agreed well with real sandstones but challenges with printing resolution and defects resulted in internal voids and printing failure [12].

Here, DLP 3D printing, which has numerous advantages over FFF (including print resolution [13,14]), is explored for fabricating reactive porous media containing calcite. Photosensitive resin is mixed with varying calcite volume percentages and pore structures of a real sandstone sample printed. The resulting printed samples analyzed using μCT imaging.

2 Methodology

Commercial ANYCUBIC resin (density 1.1g/cm^3) was used. Iceland spar calcite crystals were crushed manually and sieved through a 90μm mesh, captured on a 63μm mesh. This particle size range is detectable by μCT while not interfering with the printing process. Calcite powder and resin were combined and thoroughly mixed in a beaker at varied calcite volume fractions of 3, 5, and 7v%. Calcite content was determined gravimetrically based on the density of calcite (2.71g/cm^3)[15].

A 3D Bentheimer sandstone μCT image was downloaded from Digital Rock Portal [16]. The image was cropped, denoised using a median filter, segmented to grains and pores, and the selected region of interest (grain) converted into a 3D mesh in Dragonfly. The mesh was enlarged 20x to match the 3D printer resolution and exported as a (.stl) file.

An ANYCUBIC Photon 3D DLP printer was used. The 3D model was sliced into 25µm layers using Photon Workshop V2.1.26 and printed at 45º with supports (~6 hr print time). The 7v% calcite mixture was also printed at 50µm layer thickness (~3 hr print time). After printing, supports were removed, and the object washed using 70v% isopropyl alcohol and deionized water to remove excess resin followed by a 10 minute UV chamber post-cure.

Printed samples were imaged with µCT using a Zeiss Xradia 620 Versa 3D microscope at a resolution of 12.5µm. Images were processed and analyzed to determine porosity, calcite volume fraction, total and calcite accessible surface area, and normalized calcite surface area (details in supplementary information).

Printed sample reactivity was examined in batch experiments. A sample without calcite and the 5v% calcite sample were immersed in pH 3.5 HCl solutions at room temperature (18°C) and pH monitored. Calcium concentration was measured in the final solution using ICP-OES.

3 Results

3D µCT images of the Bentheimer sandstone, resulting mesh, and 20x magnified 3D printed sample with 5v% calcite are shown in Figure 1. The mesh porosity is 21.83% while the reported porosity from the original µCT image is 22.64% [16].

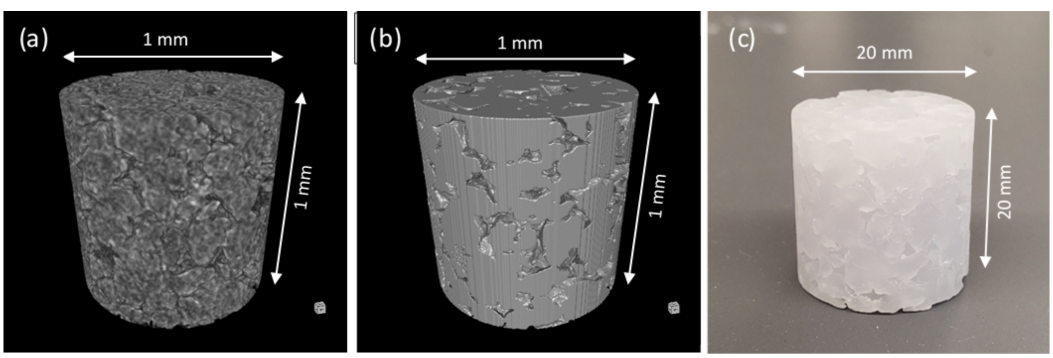

Figure 1 (a) µCT image of Bentheimer sample, (b) generated 3D mesh, and (c) 20x magnification printed sample with 5v% calcite.

µCT images of the printed samples are shown in Figure 2(a-f) and analyzed properties given in Table 1. The printed sample porosities are very consistent; 18.9%, 18.5% and 18.2%, respectively (standard deviation of 0.28%), indicating minimal variation. This is good agreement with the generated model porosity (21.8 %), similar to the difference seen in other studies [17,18] likely due to trapping of resin in the micropores [18].

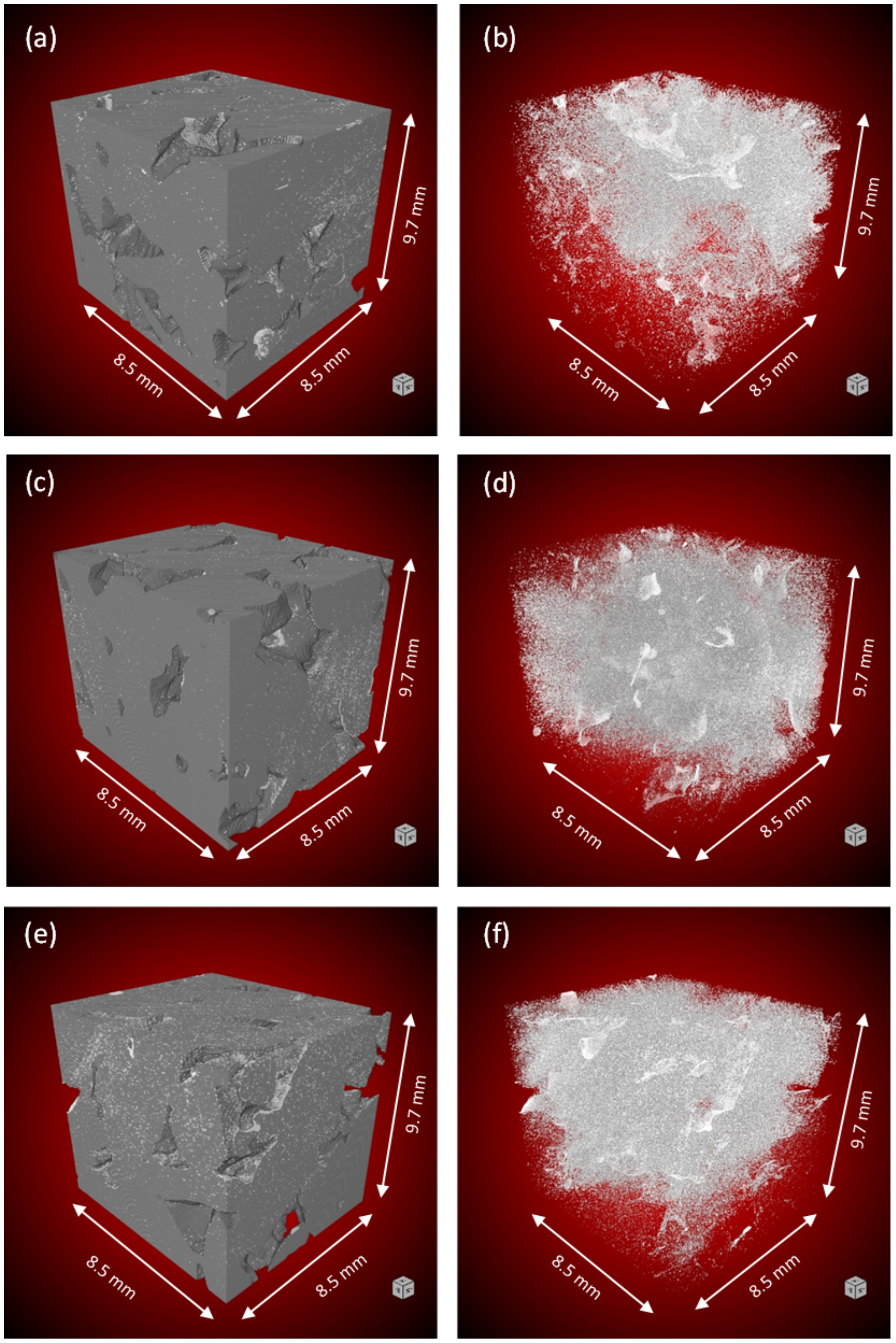

Figure 2 Segmented μCT images of calcite (white) and polymer (gray) for the (a) 3v%, (c) 5v%, and (e) 7v%. Segmented calcite particle distribution in (b) 3v%, (d) 5v%, and (f) 7v%.

The 3 and 5v% samples contain 2.76v% and 4.52v% calcite, respectively; in good agreement with the resin calcite content. The 7v% calcite sample, however, only contains 2.52v% calcite, significantly less than in the resin mixture. This is attributed to particle agglomeration and settling, promoted by the large calcite content. To prevent this behavior, a sample was printed with 7v% calcite using a 50 μm layer thickness (reduced printing time). This significantly increased the calcite volume fraction (4.62v%) while maintaining the target porosity. However, further optimization is needed for printing samples with targeted higher calcite contents.

From printed sample images, calcite is present throughout the sample (Figure 2(b,d,f)) with some surface clumps observed. Calcite accessibility, defined as calcite on the surface of the structure and accessible to reactive fluids, is quantified from the images (Table 1). Only a fraction of the calcite present is accessible, 5.39%, 10.22% and 6.28% for 3, 5, and 7v% samples.

Table 1 Sample Properties Extracted from μCT Images of 3-D Printed Samples

Sample Property	3v% calcite	5v% calcite	7v% calcite	7v% calcite
Calcite in resin mixture (v%)	3	5	7	7
Printing layer thickness(μm)	25	25	25	50
Polymer in printed sample (v%)	97.24	95.48	97.48	95.42
Calcite in printed sample (v%)	2.76	4.52	2.52	4.57
Porosity of printed sample	18.9 %	18.5 %	18.2 %	18.2 %
Calcite accessibility (%)	5.39	10.22	6.28	8.85
Polymer accessibility (%)	94.61	89.78	93.72	91.15
Total surface area (m^2) ($x10^{-4}$)	5.12	6.00	5.36	5.76
Calcite accessible surface area (m^2) ($x10^{-5}$)	2.76	6.13	3.37	5.10
Calcite in printed sample (g)	0.038	0.062	0.034	0.062
Normalized accessible calcite surface area (m^2/g) ($x10^{-4}$)	7.35	9.96	9.82	8.20

Porous media reaction rates are largely controlled by reactive surface area. The total surface area, calcite accessible surface area, and normalized accessible calcite surface area extracted from printed sample images are in Table 1. Total accessible surface areas are similar, indicating good agreement between the 3D printed pore structures. Slightly larger variations are found for calcite accessible surface area, though within one order of magnitude, between samples.

The utility of this approach for reflecting porous media reactivity was probed by comparing accessible calcite surface area with those quantified for actual sandstones, where good agreement is found in comparison with a Paluxy sandstone (8.13×10^{-4} m^2/g) [19]. Normalized calcite surface areas are an order of magnitude higher than the 2.14×10^{-5} m^2/g quantified for a 0.03v% calcite volcanogenic sandstone sample, though lower accessible surface area for that sample is possibly a result of clay coatings [20].

Batch acid dissolution experiments showed no pH change (Figure 3) or dissolved calcium for the sample without calcite, whereas the 5v% calcite sample showed both a pH increase over 4 days (Figure 3) and a calcium solution concentration of 5.15mg/L.

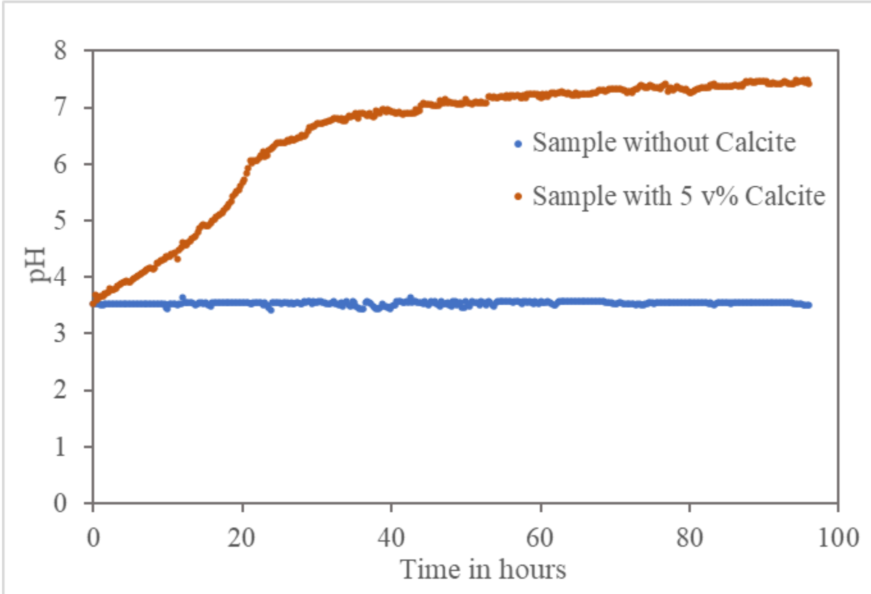

Figure 3 pH evolution for 3D printed samples.

5 Conclusions

DLP 3D printing of reactive porous media was demonstrated where printed samples reflected the reactive properties of real samples through inclusion of calcite within the resin at varied amounts. 3D images of printed samples found calcite content to increase with the resin calcite content, though for the highest volume fraction (7v%) particle settling reduced calcite content in the printed specimen. Improvement (83%) in calcite content for the 7v% was achieved by reducing printing time through a larger layer thickness (50μm). With regards to reproducibly replicating porous media characteristics, the extracted porosity were reproducible (standard deviation of 0.28%) and the normalized calcite accessible surface areas agree well with real sandstone samples. Furthermore, calcite dissolution during the batch experiment validated the reactivity of surface present calcite. Overall, DLP printing is a viable means to fabricate replicable reactive porous media.

Declaration of Competing Interest

The authors declare that they have no known competing financial interests or personal relationships that could have appeared to influence the work reported in this paper.

Acknowledgments

This work is supported by Auburn University (AU) and the National Science Foundation under grant No. 2025626. 3D images obtained using a μCT instrument purchased using NSF grant No. 19198181. The authors thank Jessica Brouillette, an AU undergraduate student, for her assistance during 3D printing.

References

1. Bacher, M., Schwen, A., & Koestel, J. (2015). Three-dimensional printing of macropore networks of an undisturbed soil sample. *Vadose Zone Journal*, *14*(2), vzj2014-08.
2. Dal Ferro, N., & Morari, F. (2015). From real soils to 3D-printed soils: reproduction of

complex pore network at the real size in a silty-loam soil. *Soil Science Society of America*.

3. Ishutov, S., Hasiuk, F. J., Jobe, D., & Agar, S. (2018). Using resin‐based 3D printing to build geometrically accurate proxies of porous sedimentary rocks. *Groundwater*, *56*(3), 482–490.
4. Kong, L., Ostadhassan, M., Hou, X., Mann, M., & Li, C. (2019). Microstructure characteristics and fractal analysis of 3D-printed sandstone using micro-CT and SEM-EDS. *Journal of Petroleum Science and Engineering*, *175*, 1039–1048.
5. Head, D., & Vanorio, T. (2016). Effects of changes in rock microstructures on permeability: 3‐D printing investigation. *Geophysical Research Letters*, *43*(14), 7494–7502.
6. Hodder, K. J., Nychka, J. A., & Chalaturnyk, R. J. (2018). Process limitations of 3D printing model rock. *Progress in Additive Manufacturing*, *3*(3), 173–182.
7. Jiang, C., & Zhao, G.-F. (2015). A preliminary study of 3D printing on rock mechanics. *Rock Mechanics and Rock Engineering*, *48*(3), 1041–1050.
8. Yang, L., Xu, T., Yang, B., Tian, H., & Lei, H. (2014). Effects of mineral composition and heterogeneity on the reservoir quality evolution with CO2 intrusion. *Geochemistry, Geophysics, Geosystems*, *15*(3), 605–618.
9. Almetwally, A. G., & Jabbari, H. (2019). CT-scan image processing for accurate pore network modeling and core samples 3D printing: polynomial interpolation & geostatistical QC. *53rd US Rock Mechanics/Geomechanics Symposium*.
10. Xu, W., Jambhulkar, S., Zhu, Y., Ravichandran, D., Kakarla, M., Vernon, B., Lott, D.G., Cornella, J.L., Shefi, O., Miquelard-Garnier, G. and Yang, Y., 2021. 3D printing for polymer/particle-based processing: A review. Composites Part B: Engineering, 223, p.109102.
11. Shinde, V.V., Celestine, A.D., Beckingham, L.E., & Beckingham, B.S. (2020). Stereolithography 3D printing of microcapsule catalyst-based self-healing composites. *ACS Applied Polymer Materials*, *2*(11), 5048-5057.
12. Anjikar, I. S., Wales, S., & Beckingham, L. E. (2020). Fused Filament Fabrication 3-D Printing of Reactive Porous Media. *Geophysical Research Letters*, *47*(9), 1–9. https://doi.org/10.1029/2020GL087665
13. Ahn, D., Stevens, L. M., Zhou, K., & Page, Z. A. (2020). Rapid high-resolution visible light 3D printing. *ACS Central Science*, *6*(9), 1555–1563.
14. Shinde, V.V., Wang, Y., Salek, Md.f., Auad, M.L., Becknigham, L.E., Beckingham, B.S., 2022. Material Design for Enhancing Properties of 3D Printed Polymer Composites for Target Applications. *Technologies*, 10(2), https://doi.org/10.3390/technologies10020045.
15. Lambkin, D. C., Gwilliam, K. H., Layton, C., Canti, M. G., Piearce, T. G., & Hodson, M. E. (2011). Production and dissolution rates of earthworm-secreted calcium carbonate. *Pedobiologia*, *54*, S119–S129. https://doi.org/https://doi.org/10.1016/j.pedobi.2011.09.003
16. Neumann, R., Andreeta, M., & Lucas-Oliveira, E. (2020). *11 Sandstones: raw, filtered and segmented data*. www.digitalrocksportal.org
17. Ishutov, S., Hasiuk, F. J., Harding, C., & Gray, J. N. (2015). 3D printing sandstone porosity models. *Interpretation*, *3*(3), SX49–SX61.
18. Song, R., Wang, Y., Sun, S., & Liu, J. (2021). Characterization and microfabrication of natural porous rocks: from micro-CT imaging and digital rock modelling to micro-3D-

printed rock analogs. *Journal of Petroleum Science and Engineering*, 108827.

19. Qin, F. and Beckingham, L.E., 2019. Impact of image resolution on quantification of mineral abundances and accessible surface areas. *Chemical Geology*, *523*, pp.31-41.
20. Beckingham, L.E., Mitnick, E.H., Steefel, C.I., Zhang, S., Voltolini, M., Swift, A.M., Yang, L., Cole, D.R., Sheets, J.M., Ajo-Franklin, J.B. and DePaolo, D.J., 2016. Evaluation of mineral reactive surface area estimates for prediction of reactivity of a multi-mineral sediment. *Geochimica et Cosmochimica Acta*, *188*, pp.310-329.